HAL
open science

Shape-selective purification of gold nanorods with low aspect ratio using a simple centrifugation method

Maxime Boksebeld, Nicholas Blanchard, Ali Jaffal, Yann Chevolot, Virginie Monnier

To cite this version:

Maxime Boksebeld, Nicholas Blanchard, Ali Jaffal, Yann Chevolot, Virginie Monnier. Shape-selective purification of gold nanorods with low aspect ratio using a simple centrifugation method. Gold Bulletin : The journal of gold science, technology and applications , 2017, 50 (1), pp.69-76. 10.1007/s13404-017-0197-9 . hal-01701524

HAL Id: hal-01701524

https://hal.science/hal-01701524v1

Submitted on 3 Apr 2018

HAL is a multi-disciplinary open access archive for the deposit and dissemination of scientific research documents, whether they are published or not. The documents may come from teaching and research institutions in France or abroad, or from public or private research centers.

L'archive ouverte pluridisciplinaire **HAL**, est destinée au dépôt et à la diffusion de documents scientifiques de niveau recherche, publiés ou non, émanant des établissements d'enseignement et de recherche français ou étrangers, des laboratoires publics ou privés.

Shape-selective purification of gold nanorods with low aspect ratio using a simple centrifugation method

Maxime Boksebeld, Nicholas P. Blanchard, Ali Jaffal, Yann Chevolot & Virginie Monnier

Gold Bulletin
The journal of gold science, technology and applications

ISSN 2364-821X
Volume 50
Number 1

Gold Bull (2017) 50:69-76
DOI 10.1007/s13404-017-0197-9

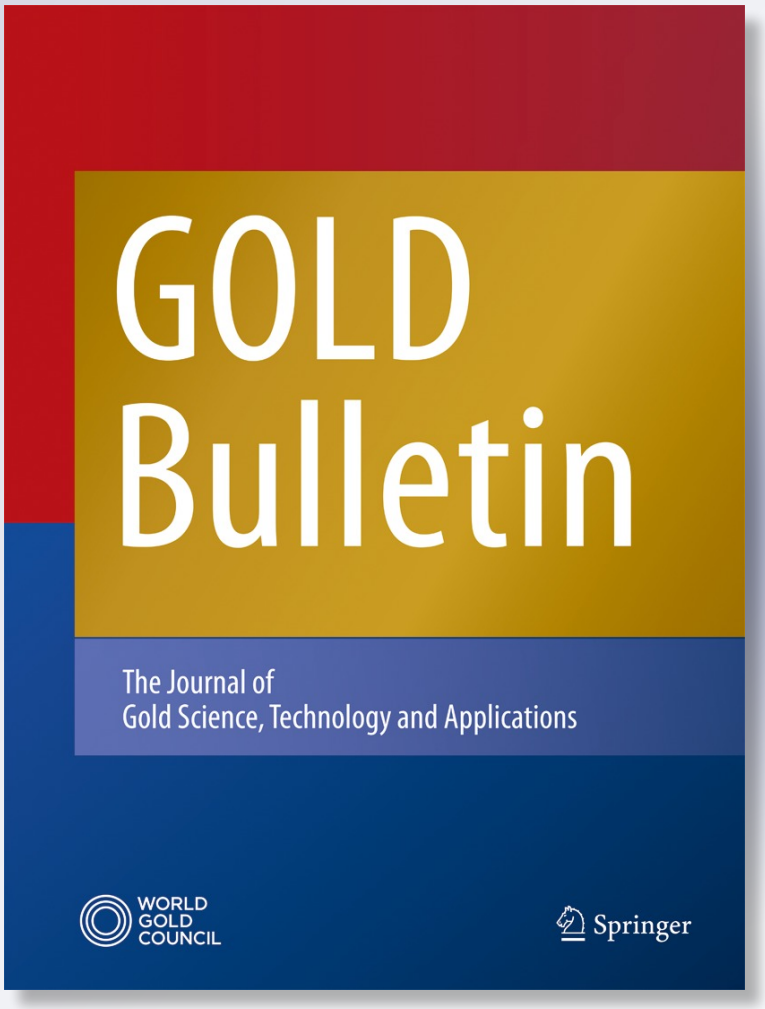

Springer

Your article is protected by copyright and all rights are held exclusively by Springer International Publishing Switzerland. This e-offprint is for personal use only and shall not be self-archived in electronic repositories. If you wish to self-archive your article, please use the accepted manuscript version for posting on your own website. You may further deposit the accepted manuscript version in any repository, provided it is only made publicly available 12 months after official publication or later and provided acknowledgement is given to the original source of publication and a link is inserted to the published article on Springer's website. The link must be accompanied by the following text: "The final publication is available at link.springer.com”.

Springer

Author's personal copy

Gold Bull (2017) 50:69–76
DOI 10.1007/s13404-017-0197-9

ORIGINAL PAPER

Shape-selective purification of gold nanorods with low aspect ratio using a simple centrifugation method

Maxime Boksebeld[1] · Nicholas P. Blanchard[2] · Ali Jaffal[1] · Yann Chevolot[1] · Virginie Monnier[1]

Received: 6 September 2016 / Accepted: 11 January 2017 / Published online: 27 January 2017
© Springer International Publishing Switzerland 2017

Abstract This work presents a new and simple procedure for the shape selective purification of gold nanorods from a mixture of rods and spheres. Previously reported methods were time-consuming and revealed several drawbacks such as low yields and difficulty to recover the purified nanoparticles. Additionally, they were mostly applied to high aspect ratio (AR) nanorods. Our process is based on only simple and short centrifugation steps in order to precipitate specifically gold nanospheres. Samples containing low AR nanorods (AR < 6) were selected to perform the purification process. The supernatant content was followed by UV-Visible absorption spectroscopy after each centrifugation step. Then, transmission electron microscopy (TEM) allowed extract the purification efficiency thanks to shape analyses performed on more than 1000 nanoparticles. These results showed that our centrifugation process was applied successfully to three sizes of nanorods (2.4, 3.7, and 5.3). High purification yields of 72 and 78% were attained for AR = 3.7 and AR = 5.3 nanorods, respectively.

Keywords Gold · Nanorods · Shape selective · Centrifugation · Purification

Electronic supplementary material The online version of this article (doi:10.1007/s13404-017-0197-9) contains supplementary material, which is available to authorized users.

✉ Virginie Monnier
virginie.monnier@ec-lyon.fr

[1] Institut des nanotechnologies de Lyon, Ecole Centrale de Lyon, Université de Lyon, 36 Avenue Guy de Collongue, F-69134 Ecully, France

[2] CNRS, Institut Lumière Matière, Université de Lyon, Université Claude Bernard Lyon 1, F-69622 Lyon, France

Introduction

The interest of gold nanoparticles for applications in the biological sciences has considerably increased over the last decades, principally due to numerous advantageous properties, in particular localized plasmon resonance [1–3] and good biocompatibility [4–6]. Plasmonic properties are valuable in many applications such as the enhancement of optical signals used for biomedical diagnosis (fluorescence [7–9], Raman [10–13], two-photon excited fluorescence [14–16], second harmonic generation [17, 18]) or photothermic/photodynamic properties for light-triggered phototherapy [19–23]. In addition, the good biocompatibility of gold nanoparticles makes them suitable in applications such as in vivo imaging, diagnosis, or therapy.

Gold nanoparticle synthesis has been widely studied. Among all the different methods, the most popular one is based on the reduction of a gold salt ($HAuCl_4$) by sodium citrate [24]. The Frens' protocol [25] offers a simple and reproducible synthesis of small and monodisperse gold nanospheres with a diameter lower than 60 nm. These spherical nanoparticles exhibit strong plasmonic properties in the visible range with a plasmon band close to 525 nm. However, for many applications, the plasmon band needs to be shifted to longer wavelengths. For example, in biological imaging, it is useful to use gold nanoparticles with a plasmon band located in the near infrared region as this corresponds to the transparency window of living tissues [26].

To achieve this, different choices can be considered such as shape or size tuning [27]. One of the most studied solutions is the synthesis of gold nanorods which exhibit strong and tunable plasmon bands from 600 to 1600 nm [28–30]. Different kinds of synthesis methods have been

Author's personal copy

described. In these different syntheses, it is common to observe a significant amount of nanospheres as a synthesis by-product. These nanospheres can represent between 10 and 90% of the total amount of nanoparticles [31, 32].

Most of the time, these nanospheres are ignored and the nanorods are used directly. However, for some applications, the presence of nanospheres can be a problem. For example, it is known that cellular uptake of nanoparticles is strongly influenced by their shape [4, 33]. Thus, there is an interest to remove specifically nanospheres from gold nanorod samples.

Some studies on gold nanorod purification have already been realized. Different methods have been proposed such as size-exclusion chromatography (SEC) [34] or centrifugation/precipitation-based methods [31, 32, 35]. However, all these methods showed limitations.

SEC is limited because of the irreversible adsorption of nanoparticles in the stationary phase. The addition of high amounts of surfactants (≈50 mM) can reduce this problem. Nevertheless, the nanoparticle fractions obtained by SEC purification are generally highly diluted. In addition, SEC has only been applied to nanorods with high aspect ratio (AR > 10). Indeed, for nanorods with a low aspect ratio, shape differences may be not sufficient to ensure an effective shape separation.

Jana [32] and Khanal [35] proposed using precipitation-based techniques to purify gold nanorods. On one hand, Jana et al. reported the separation of long nanorods (AR > 15–20) using a hot and concentrated cetyl trimethylammonium bromide (CTAB) aqueous solution (0.1 M). In their work, hot CTAB was used to stabilize all the nanoparticles, while cold CTAB could not stabilize the longest nanorods, inducing their specific sedimentation. On the other hand, Khanal et al. proposed to induce an autoassembly of long nanorods (AR > 15–20) in the presence of concentrated CTAB (0.1 M) and then allow these nanorods assemblies to sediment over 10 to 12 h. The efficiency of these techniques was demonstrated, but the authors did not show results for low aspect ratio nanorods (AR < 10). Moreover, the addition of an excess of CTAB to the nanorods can be a problem for potential applications. Indeed, as CTAB is hard to remove from nanorods' surface, further functionalization steps can be difficult to perform.

For these reasons, methods using simple centrifugation processes present a great interest.

Sharma et al. [31] proposed using a single long centrifugation step (5600 g, 30 min) to separate gold nanorods (AR = 7.3) from gold nanospheres owing to the difference of sedimentation coefficient between these two types of nanoparticles. After centrifugation, it was observed that gold nanorods were preferentially located on the side walls of the centrifugation tubes, whereas gold nanospheres were located at the bottom. Thus, it is possible to use centrifugation to separate two populations of nanoparticles. Due to the vicinity of the two precipitates, the remaining problem is to recover these purified nanorods on the side walls of the centrifugation tube as unfortunately they can be easily remixed with nanospheres during their extraction. Moreover, during precipitation, irreversible aggregation of the nanorods can occur, leading to a degradation of their plasmonic properties.

In this work, we propose to go further, improving Sharma's protocol, using three short centrifugation steps (6700*g*, 3 × 1 min) to precipitate, specifically and only, gold nanospheres in order to simplify the purification process. Indeed, using our protocol, nanorods remain in the supernatant; thus, they are easier to extract. In addition, under our conditions, the nanorods do not aggregate as they remain in the supernatant. Finally, we chose to use nanorods with low aspect ratios (AR < 6), considering this case as the less favorable to perform shape-selective separation. The optical and structural properties of nanorods samples were investigated by UV-visible absorption spectroscopy and transmission electron microscopy (TEM) imaging, before purification and after several centrifugation steps. Three nanorod aspect ratios (AR = 2.4, AR = 3.7 and AR = 5.3) were selected. Their capacity to be separated from nanospheres was evaluated and compared.

Experimental

Nanorods synthesis

All chemicals were obtained from Sigma-Aldrich and used as received. Milli-Q water (18.2 MΩ/cm) was used in all the preparations. Nanorods were prepared using a previously reported protocol [30]. Gold seeds were synthesized by mixing 629 μL of aqueous CTAB solution (150 mM), 216 μL of deionized water and 55.1 μL of aqueous $HAuCl_4$ solution (4.28 mM). Then, 100 μL of $NaBH_4$ aqueous solution was added and the obtained solution was left to react during 3 h at 25 °C. Next, the growth solution was prepared by mixing 9.87 mL of aqueous CTAB solution (150 mM), 2.2 mL of deionized water, and 1.73 mL of aqueous $HAuCl_4$ solution (4.28 mM). Then, 32, 130, or 160 μL of an aqueous $AgNO_3$ solution (7.4 mM) were added, to obtain nanorods with AR = 2.4, 3.7, and 5.3, respectively. The obtained solution was stirred slowly during 2 min, and 1 mL of aqueous solution of ascorbic acid (8.18 mM) was then added. After a slow stirring of 1 min, 25 μL of the previously prepared gold seed suspension was added. The solution was stirred for 1 min and let to react, at 30 °C, overnight. Centrifugation

Author's personal copy

Table 1 Size characteristics of the studied samples

AR	2.4	3.7	5.3
Nanorod diameter (nm)	18.9 ± 1.4	11.5 ± 0.5	9.9 ± 1.1
Nanorod length (nm)	45.2 ± 1.9	42.8 ± 1.8	52.8 ± 3.5
Nanosphere diameter (nm)	Bimodal	Bimodal	Bimodal
	25.3±2.1	22.0 ± 1.2	20.6 ± 0.9
	47.4 ± 1.7	38.0 ± 2.7	46.1 ± 3.8

at 6700*g* during 5 min was used to stop the reaction and remove reactants and by-products from nanorod suspension after reaction.

Nanorods shape-selective purification

Nanorod suspensions were centrifuged at 6700*g* during 1 min. Supernatants, containing gold nanorods, were recovered and precipitates containing nanospheres were discarded. Supernatants were centrifuged with the same conditions and the precipitates were again discarded. Supernatants were centrifuged a third time, with the same conditions, and precipitates were discarded. Supernatants were analyzed using UV-visible absorption spectroscopy and TEM.

Characterization methods

UV-visible absorption spectroscopy was performed on a double beam SAFAS mc2 spectrophotometer using quartz cuvettes. TEM images were realized with a JEOL 2100HT working at 200 kV. For TEM studies, 2 μL of the diluted dispersion of nanoparticles was deposited onto a carbon holey grid (Ted Pella, Inc.). Images were analyzed with ImageJ 1.46r software. Histograms were obtained on a population of at least 100 nanoparticles. For nanosphere percentage calculation, analyses were performed on 1000 nanoparticles coming from at least eight different TEM images in order to obtain representative statistical data.

Results and discussion

Three nanorod samples were prepared using various amounts of silver nitrate in order to obtain different aspect ratios. Silver ions combined with CTAB allow the anisotropic growth of the nanorods to be controlled. TEM was used to characterize the as-synthesized samples. Images and corresponding size distributions are given in the Supporting Information. The size characteristics of the samples are summarized in Table 1. Nanorods with increasing aspect ratios exhibit decreasing diameters, from 18.9 to 9.9 nm. Their lengths range between 42.8 and 52.8 nm. As shown in TEM images (Figs. S1, S2, and S3 in the Supporting Information), numerous nanospheres can be observed in all samples. In all cases, their size distribution is bimodal, with a first population of nanospheres whose mean diameter is between 20.6 and 25.3 nm and a second population between 38.0 and 47.4 nm of diameter. For all populations of nanoparticles, the standard deviation was found to be not higher than 10%.

Nanorods were separated from nanospheres using successive centrifugation steps. Nanorods were recovered in the supernatants, while nanospheres were precipitated to the bottom of centrifugation tubes. The mass to surface ratio was selected to compare nanoparticles theoretical sedimentation properties (Table 2). Indeed, for nanoparticles with different shapes such as nanorods and nanospheres, two parameters must be considered for sedimentation: gravitational force and friction coefficient [31]. The gravitational force is directly linked to the nanoparticles' mass: as the mass increases, the sedimentation speed increases. The friction coefficient is associated to the surface of the nanoparticles in contact with the

Table 2 Calculated mass and surface of nanospheres and nanorods

AR		2.4	3.7	5.3
Smaller nanospheres	Mass (10^{-18} g)	166	109	90
	Surface (nm^2)	2011	1520	1333
	Mass to surface ratio (g m^{-2})	0.082	0.071	0.067
Bigger nanospheres	Mass (10^{-18} g)	1093	563	1005
	Surface (nm^2)	7058	4536	6677
	Mass to Surface Ratio (g m^{-2})	0.155	0.124	0.150
Nanorods[a]	Mass (10^{-18} g)	155	61.4	59.2
	Surface (nm^2)	2027	1302	1457
	Mass to Surface Ratio (g m^{-2})	0.076	0.047	0.041

[a] Penta-twinned nanorods [3, 39] were considered for mass and surface calculations

Author's personal copy

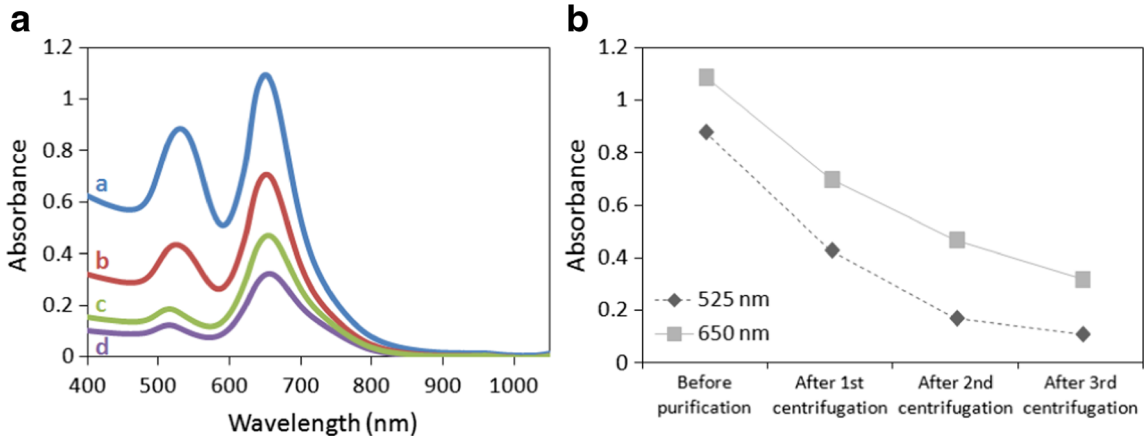

Fig. 1 **a** UV-Visible absorption spectra of gold nanorods with AR = 2.4 before purification (*a*), after the first centrifugation step (*b*), after the second centrifugation step (*c*), and after the third centrifugation step (*d*). **b** Absorbance values at λ = 525 nm (*diamond*) and λ = 650 nm (*square*) at each step

solvent. Thus, as the surface increases, the sedimentation slows down. As shown in Table 2, nanorods exhibit lower mass to surface ratios than the two populations of nanospheres. Thus, the sedimentation speed of nanorods is expected to be lower than that of nanospheres. This is consistent with our experimental observations. It is noticed in Table 2 that the difference in mass to surface ratio between nanorods and nanospheres increases for higher AR. Thus, centrifugation is supposed to be theoretically more efficient for nanorods with high AR.

The supernatants containing nanorods after each step of centrifugation were first studied by UV-visible absorption spectroscopy and compared to the sample before purification (Figs. 1, 2, and 3). For all types of nanorod, two main peaks can be observed in the absorption spectra. The peak located at higher wavelengths is related to the longitudinal plasmon resonance mode of the nanorods. Its position is specific to the nanorods aspect ratio: It is located at λ = 650 nm, λ = 790 nm, and λ = 940 nm for nanorods with AR = 2.4 (Fig. 1a), AR = 3.7 (Fig. 2a) and AR = 5.3 (Fig. 3a), respectively. The peak around λ = 525 nm has two origins: (i) It is due to the transverse resonance mode of nanorods, and (ii) it is also associated to the plasmon resonance mode of nanospheres.

The first contribution (transverse resonance mode of nanorods) is known to be relatively small and can be neglected [34, 36]. Thus, we can assume that this peak is mainly due to nanospheres. The presence of two nanosphere populations (as detailed in Table 1) has little effect on the position of the plasmon band. Indeed, for nanosphere diameters ranging from 5 to 50 nm, the plasmon band is still between λ = 520 nm and λ = 530 nm. Therefore, the absorbance value at λ = 525 nm can be a means to evaluate the presence of nanospheres in each

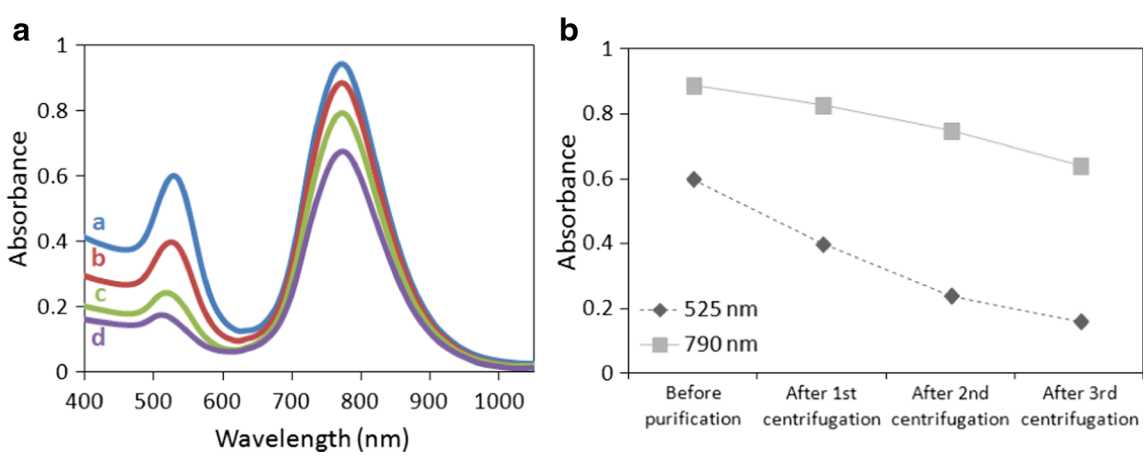

Fig. 2 **a** UV-Visible absorption spectra of gold nanorods with AR = 3.7 before purification (*a*), after the first centrifugation step (*b*), after the second centrifugation step (*c*), and after the third centrifugation step (*d*). **b** Absorbance values at λ = 525 nm (*diamond*) and λ = 790 nm (*square*) at each step

Author's personal copy

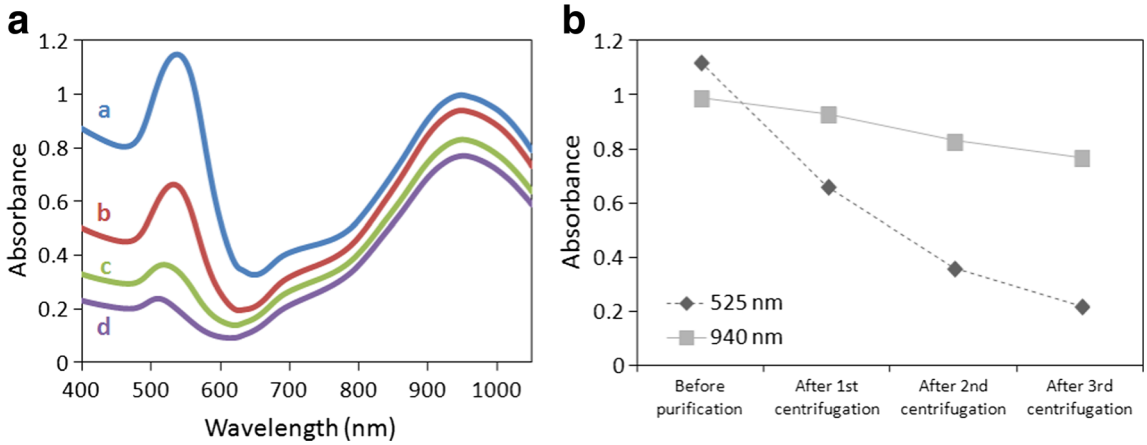

Fig. 3 **a** UV-Visible absorption spectra of gold nanorods with AR = 5.3 before purification (*a*), after the first centrifugation step (*b*), after the second centrifugation step (*c*), and after the third centrifugation step (*d*). **b** Absorbance values at λ = 525 nm (*diamond*) and λ = 940 nm (*square*) at each step

sample. The evolution of plasmon band intensities along the purification steps is presented in Figs. 1b, 2b, 3b. A strong decrease of absorbance at 525 nm can be observed for nanorods of all aspect ratios. This indicates an efficient removal of nanospheres for all the samples after centrifugation. A decrease of absorbance for longitudinal resonance mode is also observed but is less significant. These spectra are very similar to the ones obtained with the other separation methods cited previously [31, 32, 34, 35]. However, our results were obtained using nanorods with low aspect ratios (AR < 6). Different authors report that the sedimentation speed is decreased for nanorods with increased aspect ratios [31, 37, 38]. Thus, for nanorods with higher aspect ratio, our shape-selective purification could be still more efficient.

In addition, by comparing the absorbance of the longitudinal plasmon band, we can estimate the purification yield, which is considerably impacted by the aspect ratio of the nanorods. For nanorods with the lowest aspect ratio (AR = 2.4), only 29% of nanorods can be recovered after the three centrifugation steps. In comparison, nanorods with higher aspect ratios present total yields of 72 and 78% for AR = 3.7 and AR = 5.3, respectively. These yields are consistent with the easier separation for the longest nanorods [31, 37, 38].

In Fig. 4, the ratio between the absorbance measured for the longitudinal resonance mode and the absorbance at λ = 525 nm has been plotted as a function of each purification step. This graphic clearly shows that the absorbance ratio increases for the three different aspect ratios and that the ratio improves as the number of centrifugation steps is increased. This confirms the efficiency of our method.

To quantify the purification efficiency, TEM images (Fig. 5) were realized on nanorod samples before and

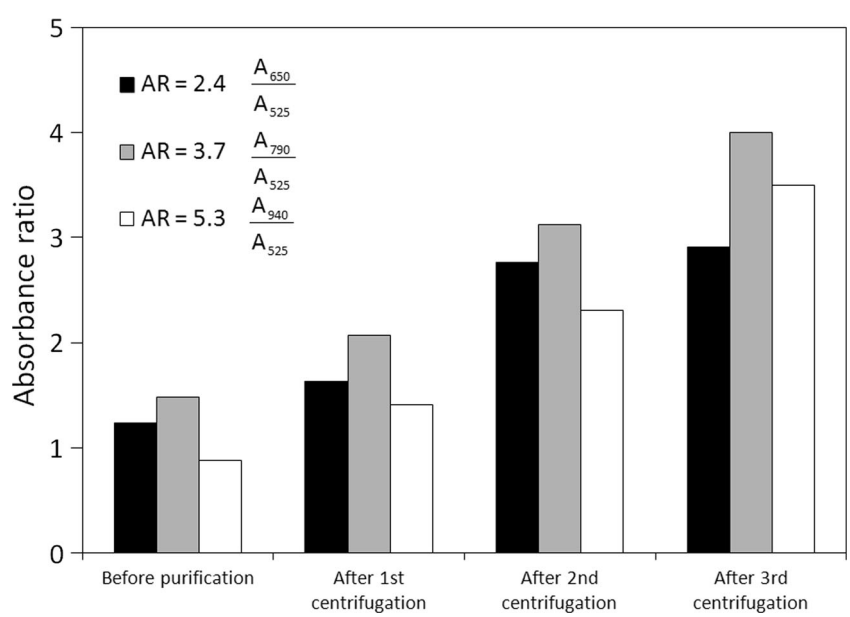

Fig. 4 Ratio between the absorbance of nanorods longitudinal resonance mode and the absorbance of nanospheres at λ = 525 nm as a function of purification steps for nanorods with AR = 2.4, A_{650}/A_{525} ratio (*black bars*), AR = 3.7, A_{790}/A_{525} ratio (*gray bar*) and AR = 5.3, A_{940}/A_{525} ratio (*white bar*)

Author's personal copy

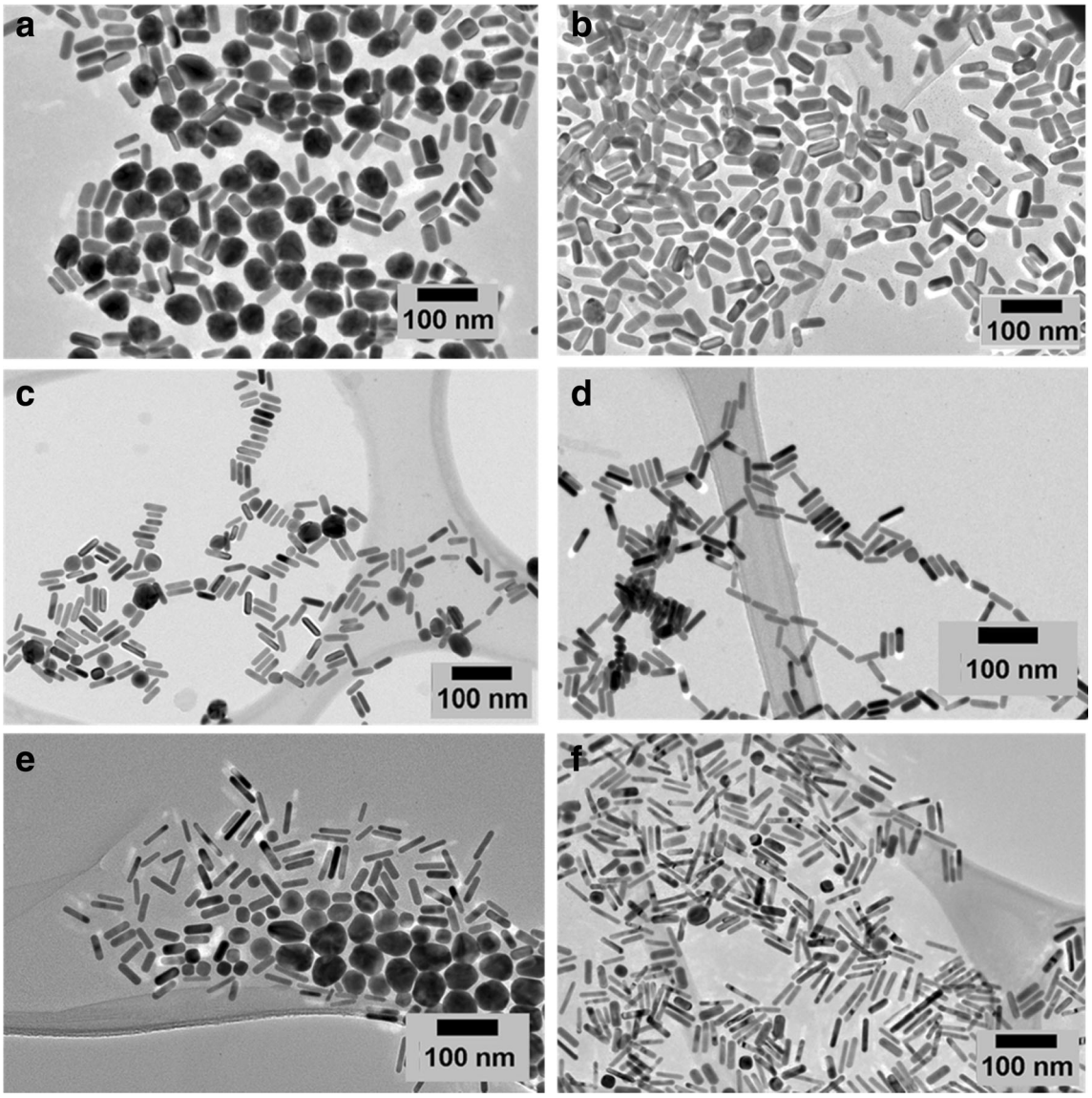

Fig. 5 TEM images of gold nanorods **a** with AR = 2.4 before purification, **b** with AR = 2.4 after the third centrifugation step, **c** with AR = 3.7 before purification, **d** with AR = 3.7 after the third centrifugation step, **e** with AR = 5.3 before purification, and **f** with AR = 5.3 after the third centrifugation step

after the three centrifugation steps. The images are consistent with the absorption spectroscopy results. Before purification, a high amount of nanospheres can be observed in the images (Fig. 5a, c, e), while after the third centrifugation step, only a few nanospheres are present (Fig. 5b, d, f).

Finally, the percentage of nanospheres in each sample was quantified on populations of 1000 nanoparticles coming from at least eight different TEM images. Counting results are summarized in Table 3. The percentage of nanospheres before purification ranges from 24 to 28% for all the samples. After three centrifugation steps, the percentage decreases to less than 10% for all aspect ratios. Interestingly, purification efficiency increases with the gold nanorods' aspect ratio. For those with the lowest aspect ratio, the percentage of nanospheres after purification was reduced by a factor of 2.9, whereas for those with the highest aspect ratio, this reduction was 3.4. These results confirm the impact of increased aspect ratios

Table 3 Nanospheres percentage in all samples, before and after shape-selective purification

Nanorods AR	2.4	3.7	5.3
Nanospheres before purification (%)	28.1	24.0	28.0
Nanospheres after purification (%)	9.6	7.0	8.3
Gain[a]	2.9	3.4	3.4

[a] The Gain is the ratio between the percentage of nanospheres before purification and after purification

Author's personal copy

on the efficiency of shape-selective purification processes, which is consistent with the results obtained by UV-visible absorption spectroscopy.

Conclusions

In this work, gold nanorods of different aspect ratios and containing initially large amounts of nanospheres (24–28%) were purified using a shape-selective method based on simple and short centrifugation steps. After centrifugation, the nanorods remain in the supernatant and can be easily recovered. Additionally, as they do not sediment, they do not aggregate and their initial plasmonic properties are preserved. This method was less efficient for low aspect ratio nanorods. Thus, it could be difficult to apply for samples containing nanorods with very low aspect ratio, for which the shape does not differ a lot from the shape of nanospheres. However, our process demonstrates its efficiency to remove specifically nanospheres from nanorods, even with nanorods of low aspect ratios (AR < 6) and with high yields (up to 78% for nanorods with an aspect ratio of 5.3). In this way, our shape-selective separation method offers an alternative to the limitations mentioned in previous reports.

Acknowledgements This work was supported by the LABEX iMUST (ANR-10-LABX-0064) of Université de Lyon, within the program "Investissements d'Avenir" (ANR-11-IDEX-0007) operated by the French National Research Agency (ANR).

References

1. Cao J, Galbraith EK, Sun T, Grattan KTV (2012) Effective surface modification of gold nanorods for localized surface plasmon resonance-based biosensors. Sensor Actuat B-Chem 169:360–367. doi:10.1016/j.snb.2012.05.019
2. Murphy CJ, Gole AM, Hunyadi SE et al (2008) Chemical sensing and imaging with metallic nanorods. Chem Commun:544–557. doi:10.1039/b711069c
3. Huang X, Neretina S, El-Sayed MA (2009) Gold nanorods: from synthesis and properties to biological and biomedical applications. Adv Mater 21:4880–4910. doi:10.1002/adma.200802789
4. Chithrani BD, Chan WCW (2007) Elucidating the mechanism of cellular uptake and removal of protein-coated gold nanoparticles of different sizes and shapes. Nano Lett 7:1542–1550. doi:10.1021/nl070363y
5. Alkilany AM, Nagaria PK, Hexel CR et al (2009) Cellular uptake and cytotoxicity of gold nanorods: molecular origin of cytotoxicity and surface effects. Small 5:701–708. doi:10.1002/smll.200801546
6. Goodman CM, McCusker CD, Yilmaz T, Rotello VM (2004) Toxicity of gold nanoparticles functionalized with cationic and anionic side chains. Bioconjug Chem 15:897–900. doi:10.1021/bc049951i
7. Aslan K, Wu M, Lakowicz JR, Geddes CD (2007) Fluorescent Core-Shell Ag@SiO2 Nanocomposites for metal-enhanced fluorescence and single nanoparticle sensing platforms. J Am Chem Soc 129:1524–1525
8. Tovmachenko OG, Graf C, van den Heuvel DJ et al (2006) Fluorescence enhancement by metal-Core/silica-Shell nanoparticles. Adv Mater 18:91–95. doi:10.1002/adma.200500451
9. Sui N, Monnier V, Zakharko Y et al (2012) Plasmon-controlled narrower and blue-shifted fluorescence emission in (Au@SiO2)SiC nanohybrids. J Nanopart Res 14:1004. doi:10.1007/s11051-012-1004-4
10. Weitz DA, Garoff S, Gersten JI, Nitzan A (1983) The enhancement of Raman scattering, resonance Raman scattering, and fluorescence from molecules adsorbed on a rough silver surface. J Chem Phys 78:5324–5338
11. He Y, Yang L, Chen Q (2013) Surface-enhanced Raman scattering spectroscopy of dendrimer-entrapped gold nanoparticles. Surf Coat Tech 228:S137–S141. doi:10.1016/j.surfcoat.2012.07.006
12. Johansson P, Xu H, Käll M (2005) Surface-enhanced Raman scattering and fluorescence near metal nanoparticles. Phys Rev B 72: 035427. doi:10.1103/PhysRevB.72.035427
13. Sha MY, Xu H, Natan MJ, Cromer R (2008) Surface-enhanced Raman scattering tags for rapid and homogeneous detection of circulating tumor cells in the presence of human whole blood. J Am Chem Soc 130:17214–17215. doi:10.1021/ja804494m
14. Li JL, Gu M (2010) Surface plasmonic gold nanorods for enhanced two-photon microscopic imaging and apoptosis induction of cancer cells. Biomaterials 31:9492–9498. doi:10.1016/j.biomaterials.2010.08.068
15. Gryczynski I, Malicka J, Shen Y et al (2002) Multiphoton excitation of fluorescence near metallic particles: enhanced and localized excitation. J Phys Chem B 106:2191–2195. doi:10.1021/jp013013n
16. Zhang T, Lu G, Shen H et al (2014) Plasmonic-enhanced two-photon fluorescence with single gold nanoshell. Sci China Ser G 57: 1038–1045. doi:10.1007/s11433-014-5460-y
17. Richter J, Steinbrück A, Pertsch T et al (2012) Plasmonic Core–Shell nanowires for enhanced second-harmonic generation. Plasmonics 8:115–120. doi:10.1007/s11468-012-9429-2
18. Richter J, Steinbrück A, Zilk M et al (2014) Core-shell potassium niobate nanowires for enhanced nonlinear optical effects. Nanoscale 6:5200–5207. doi:10.1039/c3nr05685f
19. Huang X, El-Sayed IH, Qian W, El-Sayed MA (2006) Cancer cell imaging and photothermal therapy in the near-infrared region by using gold nanorods. J Am Chem Soc 128:2115–2120
20. Kuo WS, Chang CN, Chang YT et al (2010) Gold nanorods in photodynamic therapy, as hyperthermia agents, and in near-infrared optical imaging. Angew Chem Int Ed 122:2771–2775. doi:10.1002/ange.200906927
21. Dickerson EB, Dreaden EC, Huang X et al (2008) Gold nanorod assisted near-infrared plasmonic photothermal therapy (PPTT) of squamous cell carcinoma in mice. Cancer Lett 269:57–66. doi:10.1016/j.canlet.2008.04.026
22. Vankayala R, Huang YK, Kalluru P et al (2014) First demonstration of gold nanorods-mediated photodynamic therapeutic destruction of tumors via near infra-red light activation. Small 10:1612–1622. doi:10.1002/smll.201302719
23. Kannadorai RK, Chiew GGY, Luo KQ, Liu Q (2015) Dual functions of gold nanorods as photothermal agent and autofluorescence enhancer to track cell death during plasmonic photothermal therapy. Cancer Lett 357:152–159. doi:10.1016/j.canlet.2014.11.022
24. Turkevich J, Stevenson PC, Hillier J (1951) A study of the nucleation and growth processes in the synthesis of colloidal gold. Discuss Faraday Soc 11:55–75
25. Frens G (1973) Controlled nucleation for the regulation of the particle size in monodisperse gold suspensions. Nat Phys Sci 241:20–22
26. Bonacina L (2013) Nonlinear nanomedecine: harmonic nanoparticles toward targeted diagnosis and therapy. Mol Pharmaceut 10: 783–792. doi:10.1021/mp300523e

Author's personal copy

27. Taleb A, Petit C, Pileni MP (1997) Synthesis of highly synthesis of highly monodisperse silver nanoparticles from AOT reverse micelles: a way to 2D and 3D self-organization. Chem Mater 9:950–959
28. Jana NR, Gearheart L, Murphy CJ (2001) Seed-mediated growth approach for shape-controlled synthesis of spheroidal and rod-like gold nanoparticles using a surfactant template. Adv Mater 13:1389–1393
29. Jana NR (2005) Gram-scale synthesis of soluble, near-monodisperse gold nanorods and other anisotropic nanoparticles. Small 1:875–882. doi:10.1002/smll.200500014
30. Nikoobakht B, El-Sayed MA (2003) Preparation and growth mechanism of gold nanorods (NRs) using seed-mediated growth method. Chem Mater 15:1957–1962
31. Sharma V, Park K, Srinivasarao M (2009) Shape separation of gold nanorods using centrifugation. P Natl Acad Sci USA 106:4981–4985. doi:10.1073/pnas.0800599106
32. Jana NR, Rammohun R, Mahavidyalaya R (2003) Nanorod shape separation using surfactant assisted self-assembly. Chem Commun 1950–1951
33. Chithrani BD, Ghazani AA, Chan WCW (2006) Determining the size and shape dependence of gold nanoparticle uptake into mammalian cells. Nano Lett 6:662–668. doi:10.1021/nl052396o
34. Wei GT, Liu FK, Wang CR (1999) Shape separation of nanometer gold particles by size-exclusion chromatography. Anal Chem 71: 2085–2091. doi:10.1021/ac990044u
35. Khanal BP, Zubarev ER (2010) Purification of high aspect ratio gold nanorods: complete removal of platelets. J Am Chem Soc 130:12634–12635. doi:10.1021/Ja806043p
36. Chang SS, Shih CW, Chen CD et al (1999) The shape transition of gold nanorods. Langmuir 15:701–709. doi:10.1021/la980929l
37. Dogic Z, Philipse AP, Fraden S, Dhont JKG (2000) Concentration-dependent sedimentation of colloidal rods. J Chem Phys 113:8368–8380. doi:10.1063/1.1308107
38. Peterson J (1964) Hydrodynamic alignment of rodlike macromolecules during ultra centrifugation. J Chem Phys 40:2680–2686
39. Johnson CJ, Dujardin E, Davis SA et al (2002) Growth and form of gold nanorods prepared by seed-mediated, surfactant-directed synthesis. J Mater Chem 12:1765–1770. doi:10.1039/b200953f